

# Synaptic Loss in Primary Tauopathies Revealed by [<sup>11</sup>C]UCB-J Positron Emission Tomography

Negin Holland, MRCP,<sup>1,7\*</sup> P. Simon Jones, MSc,<sup>1</sup> George Savulich, PhD,<sup>2</sup> Julie K. Wiggins, BSc,<sup>1,7</sup> Young T. Hong, PhD,<sup>1,3</sup> Tim D. Fryer, PhD,<sup>1,3</sup> Roido Manavaki, PhD,<sup>4</sup> Selena Milicevic Sephton, PhD,<sup>1,3</sup> Istvan Boros, PhD,<sup>1,3</sup> Maura Malpetti, MSc,<sup>1</sup> Frank H. Hezemans, MSc,<sup>1,6</sup> Franklin I. Aigbirhio, DPhil,<sup>1</sup> Jonathan P. Coles, FRCA, PhD,<sup>5,7</sup> John O'Brien, DM, FMedSci,<sup>2,7</sup> and James B. Rowe, FRCP, PhD<sup>1,6,7</sup>

<sup>1</sup>Department of Clinical Neurosciences, University of Cambridge, Cambridge, United Kingdom

<sup>2</sup>Department of Psychiatry, University of Cambridge, Cambridge, United Kingdom

<sup>3</sup>Wolfson Brain Imaging Centre, University of Cambridge, Cambridge, United Kingdom

<sup>4</sup>Department of Radiology, University of Cambridge, Cambridge, United Kingdom

<sup>5</sup>Division of Anaesthesia, Department of Medicine, University of Cambridge, Cambridge, United Kingdom

<sup>6</sup>Medical Research Council Cognition and Brain Sciences Unit, University of Cambridge, Cambridge, United Kingdom

<sup>7</sup>Cambridge University Hospitals NHS Foundation Trust, Cambridge, United Kingdom

**ABSTRACT: Background:** Synaptic loss is a prominent and early feature of many neurodegenerative diseases.

**Objectives:** We tested the hypothesis that synaptic density is reduced in the primary tauopathies of progressive supranuclear palsy (PSP) (Richardson's syndrome) and amyloid-negative corticobasal syndrome (CBS).

**Methods:** Forty-four participants (15 CBS, 14 PSP, and 15 age-/sex-/education-matched controls) underwent PET with the radioligand [<sup>11</sup>C]UCB-J, which binds to synaptic vesicle glycoprotein 2A, a marker of synaptic density; participants also had 3 Tesla MRI and clinical and neuropsychological assessment.

**Results:** Nine CBS patients had negative amyloid biomarkers determined by [<sup>11</sup>C]PiB PET and hence were deemed likely to have corticobasal degeneration (CBD). Patients with PSP-Richardson's syndrome and amyloid-negative CBS were impaired in executive, memory, and visuospatial tasks. [<sup>11</sup>C]UCB-J binding was reduced across frontal, temporal, parietal, and occipital lobes, cingulate, hippocampus, insula, amygdala, and subcortical structures

in both PSP and CBD patients compared to controls ( $P < 0.01$ ), with median reductions up to 50%, consistent with postmortem data. Reductions of 20% to 30% were widespread even in areas of the brain with minimal atrophy. There was a negative correlation between global [<sup>11</sup>C]UCB-J binding and the PSP and CBD rating scales ( $R = -0.61$ ,  $P < 0.002$ ;  $R = -0.72$ ,  $P < 0.001$ , respectively) and a positive correlation with the revised Addenbrooke's Cognitive Examination ( $R = 0.52$ ;  $P = 0.01$ ).

**Conclusions:** We confirm severe synaptic loss in PSP and CBD in proportion to disease severity, providing critical insight into the pathophysiology of primary degenerative tauopathies. [<sup>11</sup>C]UCB-J may facilitate treatment strategies for disease-modification, synaptic maintenance, or restoration. © 2020 The Authors. *Movement Disorders* published by Wiley Periodicals LLC. on behalf of International Parkinson and Movement Disorder Society.

**Key Words:** [<sup>11</sup>C]UCB-J PET; PSP/CBS; synaptic vesicle protein 2A; tauopathy

This is an open access article under the terms of the Creative Commons Attribution License, which permits use, distribution and reproduction in any medium, provided the original work is properly cited.

\*Correspondence to: Dr. Negin Holland, Department of Clinical Neurosciences, University of Cambridge, Herchel Smith Building, Cambridge Biomedical Campus, Cambridge, CB2 0SZ, United Kingdom; E-mail: nda26@cam.ac.uk

**Funding agencies:** The study was funded by the Cambridge University Centre for Parkinson-Plus, the National Institute for Health Research Cambridge Biomedical Research Centre (SUAG/004 RG91365 JBR), the Wellcome Trust (103838), and the Association of British Neurologists, Patrick Berthoud Charitable Trust (RG99368). M.P. is supported

by a Cambridge Trust Vice-Chancellor's Award & Sidney Sussex College Scholarship. F.H.H. is supported by a Cambridge Trust Vice-Chancellor's Award & Fitzwilliam College scholarship.

**Relevant conflicts of interest/financial disclosures:** Nothing to report.

Full financial disclosures and author roles may be found in the online version of this article.

**Received:** 13 April 2020; **Revised:** 26 May 2020; **Accepted:** 8 June 2020

**Published online 00 Month 2020 in Wiley Online Library (wileyonlinelibrary.com). DOI: 10.1002/mds.28188**

The primary degenerative tauopathies of progressive supranuclear palsy (PSP) and corticobasal degeneration (CBD) cause a severe combination of movement and cognitive impairment.<sup>1-4</sup> Pathologically, both are associated with a four-repeat (4R)-tauopathy.<sup>5</sup> We proposed that the neurophysiological and functional impairments in PSP and CBD are, at least in part, a consequence of synaptic loss. For example, at postmortem there is ~50% loss of cortical synapses in PSP and CBD,<sup>6,7</sup> and in vivo there is limited evidence of a ~20% loss of postsynaptic GABA<sub>A</sub> receptors as shown with [<sup>11</sup>C]flumazenil PET.<sup>8,9</sup> Indeed, abnormal physiology in pathways involved in presynaptic function have been identified from transcriptomic studies in patients with mutations in the microtubule-associated protein tau gene.<sup>10</sup> Transgenic models of tauopathies (e.g., rTg4510) confirm a synaptotoxic effect of oligomeric tau, before cell death.<sup>11,12</sup> Moreover, in other neurodegenerative dementias, such as Alzheimer's disease (AD), synaptic loss correlates better with cognitive dysfunction than atrophy.<sup>13</sup>

We therefore tested the hypothesis that PSP and CBD reduce synaptic density, in proportion to disease severity. We included patients with the classic phenotype of PSP, PSP-Richardson's syndrome, which has a high clinicopathological correlation,<sup>14</sup> and presents with postural instability, supranuclear gaze palsy, axial rigidity, and cognitive impairment.<sup>15</sup> Other phenotypes of PSP are increasingly recognized,<sup>3,16</sup> but excluded here. We include patients with corticobasal syndrome (CBS), with combinations of asymmetric rigidity, apraxia, dystonia, alien limb, and cognitive impairment.<sup>1,17</sup> In order to identify those with probable underlying CBD, it is necessary to exclude the substantial minority of CBS caused by AD pathology.<sup>18</sup> We therefore used amyloid imaging to distinguish those with CBS attributed to CBD, versus AD; we refer to this group as the CBD cohort. Both PSP and CBD are associated with cortical and subcortical atrophy on MRI<sup>19</sup>; and changes in neurophysiology and connectivity measured by magnetoencephalography and functional MRI.<sup>20-23</sup> However, functional changes are also observed in areas of the brain that are minimally atrophic.

We used PET with the radioligand, [<sup>11</sup>C]UCB-J ((R)-1-((3-(methyl-<sup>11</sup>C)pyridin-4-yl)methyl)-4-(3,4,5-trifluorophenyl)pyrrolidin-2-one).<sup>24</sup> This ligand quantifies synaptic density,<sup>25,26</sup> based on its affinity for the presynaptic vesicle glycoprotein 2A (SV2A), that is ubiquitously expressed in all brain synapses.<sup>27,28</sup> [<sup>11</sup>C]UCB-J has revealed hippocampal synaptic loss in AD, correlating with episodic memory loss and clinical dementia severity.<sup>29</sup> We sought correlations between regional [<sup>11</sup>C]UCB-J binding potentials, a metric of synaptic density, and disease severity, in terms of cognitive decline and global impairment on the PSP and CBD rating scales.

## Participants and Methods

### Participants and Study Design

Fourteen patients with PSP-Richardson's syndrome and 15 patients with CBS were recruited from a tertiary specialist clinic for PSP/CBS at the Cambridge University Centre for Parkinson-Plus (Cambridge, UK). Fifteen healthy volunteers were recruited from the UK National Institute for Health Research Join Dementia Research register. Patients had either probable PSP-Richardson's syndrome,<sup>3</sup> or both probable CBS and probable CBD.<sup>1</sup> Healthy controls and patient volunteers were initially screened by telephone; our exclusion criteria were: current or recent history (within the last 5 years) of cancer, concurrent use of the medication levetiracetam, history of ischaemic or haemorrhagic stroke evident on MRI available from the clinic, any severe physical illness or co-morbidity that limited ability to fully participate in the study, and any contraindications to performing MRI. Eligible participants were invited for a research visit where they underwent clinical and cognitive assessment including measures of disease severity (Table 1); these included a neurological examination by a clinician including the PSP and CBD rating scales, the UPDRS (motor subsection III), the Schwab and England Activities of Daily Living (SEADL) and Clinical Dementia Rating Scale (CDR); cognitive testing included the revised Addenbrooke's Cognitive Examination (ACE-R), the Mini-mental State Examination (MMSE), the Montreal Cognitive Assessment (MoCA), and the INECO frontal assessment test. Patients' carers completed the revised Cambridge Behavioural Inventory (CBI).

All participants underwent simultaneous 3 Tesla MRI and [<sup>11</sup>C]UCB-J PET. Patients with CBS also underwent amyloid PET imaging using Pittsburgh compound B ([<sup>11</sup>C]PiB), and cortical standardized uptake value ratio (SUVR; 50–70 minutes postinjection; whole cerebellum reference tissue) was determined using the Centiloid Project methodology.<sup>30</sup> Only those with a negative amyloid status, as characterized by a cortical [<sup>11</sup>C]PiB SUVR <1.21 (obtained by converting the Centiloid cutoff of 19 to SUVR using the Centiloid-to-SUVR transformation)<sup>31</sup> are included in the subsequent analysis, with the aim of excluding patients with CBS associated with Alzheimer's disease. We interpret this amyloid-negative group as having CBD, although acknowledge that other pathologies are possible.

The research protocol was approved by the local Cambridge Research Ethics Committee (REC: 18/EE/0059) and the Administration of Radioactive Substances Advisory Committee. All participants provided written informed consent in accordance with the Declaration of Helsinki.

### Neuroimaging

[<sup>11</sup>C]UCB-J was synthesized at the Radiopharmacy Unit, Wolfson Brain Imaging Centre, Cambridge

**TABLE 1.** Demographics and neuropsychological profile for each participant cohort

	Control	CBD	PSP	F (P)
M:F	7:8	7:2	7:7	ns <sup>a</sup>
Age at [ <sup>11</sup> C]UCB-J PET in years	68 (7.45)	70.56 (8.23)	72.79 (7.74)	ns
Disease duration in years	NA	3.94 (2.2)	4.28 (2.57)	ns <sup>b</sup>
Education in years	13.69 (2.66)	12.78 (3.27)	12.77 (5.43)	ns
ACE-R total (max. 100)	96.47 (2.88)	81.56 (10.83)	80.57 (15.02)	9.61 (<0.0004)
Attention_Orientation (max. 18)	17.87 (0.35)	16.89 (1.05)	16.43 (2.06)	4.11 (0.02)
Memory (max. 26)	24.53 (1.85)	20.67 (5.66)	21.43 (4.27)	3.50 (0.04)
Fluency (max. 14)	12.80 (1.15)	8.22 (2.86)	6.43 (3.44)	22.81 (<0.001)
Language (max. 26)	25.53 (0.92)	22.44 (5.34)	23.43 (5.21)	ns
Visuospatial (max. 16)	15.73 (0.59)	13.33 (2.55)	12.86 (3.98)	4.46 (0.02)
MMSE (max. 30)	29.27 (1.33)	26.44 (3.13)	27.00 (2.88)	4.78 (0.01)
UPDRS (max. 132)	0 (0)	38.22 (14.81)	32.36 (16.38)	ns <sup>b</sup>
PSPRS (max. 100)	0.13 (0.52)	26.78 (9.61)	29.21 (10.27)	ns <sup>b</sup>
CBDRS (max. 124)	0.20 (0.77)	29.12 (13.52)	36.80 (20.41)	ns <sup>b</sup>
MoCA (max. 30)	27.80 (1.74)	12.25 (12.96)	22.46 (2.96)	8.39 (<0.001)
INECO (max. 30)	26.00 (1.85)	14.6 0 (8.47)	17.70 (4.74)	17.22 (<0.001)
CDR sum of boxes (max. 32)	0.07 (0.26)	6.78 (4.71)	7.54 (6.55)	11.28 (<0.001)
CBI (max. 180)	2.47 (4.81)	27.44 (13.5)	42.43 (38.13)	9.97 (<0.001)
SEADL (max. 1)	0.99 (0.03)	0.56 (0.28)	0.60 (0.22)	10.54 (<0.001)

The results are given as mean (standard deviation). CBD here refers to CBS with a negative amyloid biomarker from [<sup>11</sup>C]PiB PET, and PSP refers to patients with PSP-Richardson's syndrome. The F-statistic and P values are derived from ANOVA. ns = nonsignificant at P < 0.05.

<sup>a</sup>Chi-squared test.

<sup>b</sup>ANOVA with PSP and CBD patients only.

M, male; F, female; PSPRS, Progressive Supranuclear Palsy Rating Scale; CBDRS, CBD functional rating scale; NA, nonapplicable; ANOVA, analysis of variance.

University (Cambridge, UK), using the methodology previously described.<sup>32</sup> Dynamic PET data acquisition was performed on a GE SIGNA PET/MR (GE Healthcare, Waukesha, WI) for 90 minutes, starting immediately after [<sup>11</sup>C]UCB-J injection (median injected activity: 351 ± 107 MBq; injected mass: ≤10 µg), with attenuation correction including the use of a multisubject atlas method<sup>33,34</sup> and also improvements to the MRI brain coil component.<sup>35</sup> Each emission image series was aligned using SPM12 ([www.fil.ion.ucl.ac.uk/spm/software/spm12/](http://www.fil.ion.ucl.ac.uk/spm/software/spm12/)), then rigidly registered to a T<sub>1</sub>-weighted MRI acquired during PET data acquisition (repetition time = 3.6 msec, echo time = 9.2 msec, 192 sagittal slices, in-plane resolution 0.55 × 0.55 mm [subsequently interpolated to 1.0 × 1.0 mm]; slice thickness 1.0 mm). Using a version of the Hammersmith atlas (<http://brain-development.org>) with modified posterior fossa regions, combined regions of interest (ROIs; including aggregated regions for frontal, parietal, occipital, and temporal lobes; cingulate; and cerebellum) were spatially normalized to the T<sub>1</sub>-weighted MRI of each participant using Advanced Normalization Tools (ANTs) software.<sup>36</sup> Regional time-activity curves were extracted following the application of geometric transfer matrix (GTM) partial volume correction (PVC<sup>37</sup>) to each of the dynamic PET images. ROIs were multiplied by a binary gray matter mask (>50% on the SPM12 gray matter probability map smoothed to PET spatial resolution), with the exception of the pallidum, substantia nigra, pons, and medulla because masking eliminated the ROI for some or all of the subjects. Multiple background gray matter, white matter, and cerebrospinal fluid regions were

also defined to provide whole-brain coverage for GTM PVC. The mean gray matter/(gray matter + white matter) fraction in the masked ROIs was 0.97 ± 0.03, 0.96 ± 0.03, and 0.96 ± 0.03 for the control, CBD, and PSP groups, respectively, illustrating the predominance of gray matter in the masked ROIs. To assess the impact of PVC, time-activity curves were also extracted from the same ROIs without the application of GTM PVC.

To quantify SV2A density, [<sup>11</sup>C]UCB-J nondisplaceable binding potential (BP<sub>ND</sub>) was determined, both regionally and at the voxel level, using a basis function implementation of the simplified reference tissue model,<sup>38</sup> with the reference tissue defined in the centrum semiovale.<sup>39,40</sup> The volume-weighted average of the GTM PVC BP<sub>ND</sub> values in the masked ROIs was used as a global BP<sub>ND</sub> metric. Group average BP<sub>ND</sub> images (illustrated in Fig. 1A) were obtained by spatially normalizing each individual T<sub>1</sub>-weighted MRI (and thereby the coregistered BP<sub>ND</sub> map) to Montreal Neurological Institute (MNI) space, and then to the group template using ANTs.

### Statistical Analysis

Statistical analyses used R software (version 3.6.2; R Foundation for Statistical Computing, Vienna, Austria), with analysis of covariance to compare regional [<sup>11</sup>C]UCB-J BP<sub>ND</sub> between the three groups (control, CBD, and PSP), with age as a covariate of no interest. ROIs were: frontal, temporal, parietal, and occipital lobes; cingulate cortex, hippocampus, insula, amygdala, caudate nucleus,

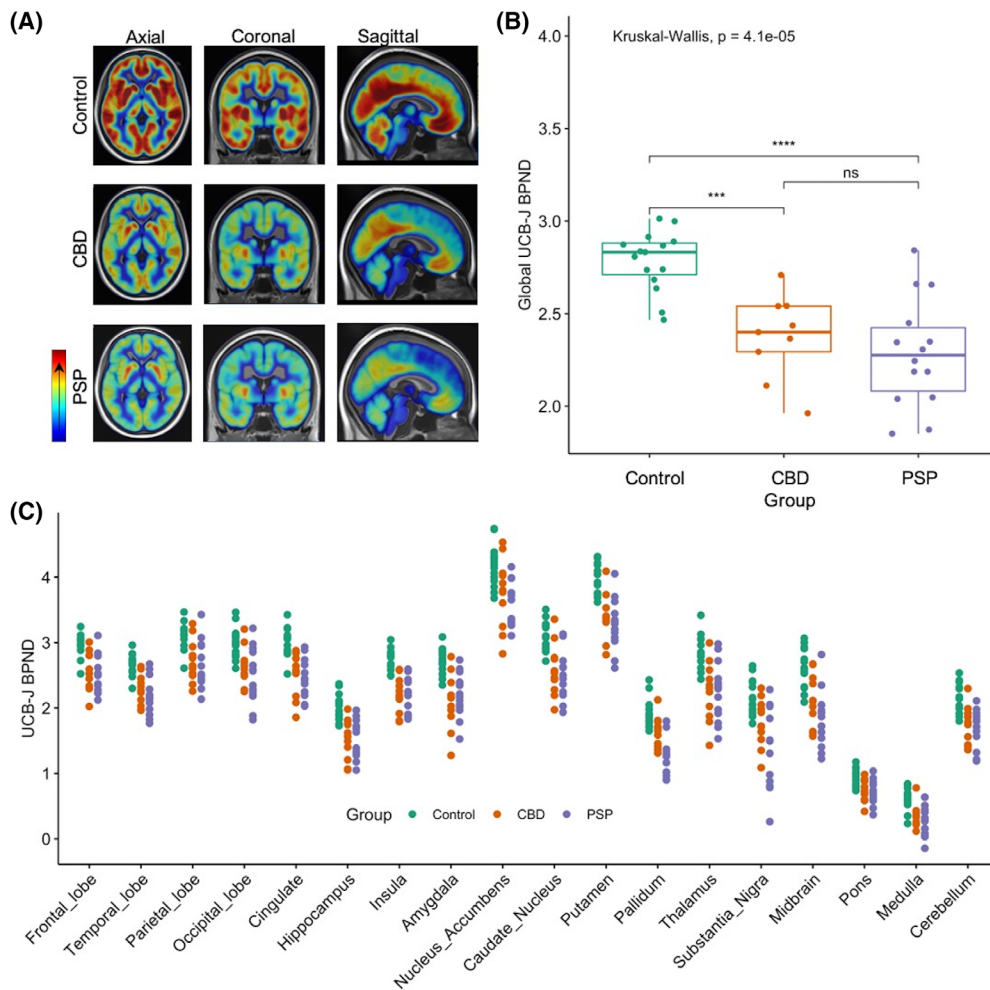


**FIG. 1.** (A) Mean [<sup>11</sup>C]UCB-J BP<sub>ND</sub> maps for control participants (top row), CBD (middle row), and PSP (bottom row); high and low BP<sub>ND</sub> values are shown by red and blue areas, respectively. (B) Reduction in global [<sup>11</sup>C]UCB-J BP<sub>ND</sub> across patients compared to controls ( $P < 0.05$ ). (C) Individual regional GTM PVC [<sup>11</sup>C]UCB-J BP<sub>ND</sub> values for control, CBD, and PSP participants, across major ROIs. Binding potential values for patients differed significantly from controls in all the regions depicted ( $P < 0.05$ , FDR corrected). CBD here refers to CBS with a negative amyloid biomarker from [<sup>11</sup>C]PiB PET, and PSP refers to patients with PSP-Richardson’s syndrome.

nucleus accumbens, putamen, pallidum, thalamus, cerebellum, substantia nigra, midbrain, pons, and medulla.

The relationships between [<sup>11</sup>C]UCB-J BP<sub>ND</sub>, disease severity (PSP and CBD rating scales), and cognition (ACE-R) were tested through linear models of the patient data, with age as a covariate of no interest.

The primary analyses used BP<sub>ND</sub> determined following GTM PVC, but all analyses were repeated using BP<sub>ND</sub> without PVC.

## Results

Of the 15 patients with CBS, 6 had a cortical [<sup>11</sup>C]PiB SUVR  $> 1.21$  and were therefore excluded from further analysis in this article. The remaining groups (9 CBD, 14 PSP, and 15 controls) were matched in age, sex, and education (Table 1). We observed typical cognitive profiles, as summarized in Table 1: Patients were impaired

on memory, verbal fluency, language, and visuospatial domains of the ACE-R, MMSE, and MoCA. There were high endorsements on the CBI, and the CDR scale, with impairment of activities of daily living on the Schwab and England scale. Concurrent medications used by our participants at the time of the [<sup>11</sup>C]UCB-J PET scan are outlined in Supporting Information Table S1. Four of our patients (1 PSP, 3 CBD) were on dopaminergic medication and 9 on amantadine (3 PSP, 6 CBD).

Compared to controls, in patients there was a significant global reduction in [<sup>11</sup>C]UCB-J BP<sub>ND</sub> (Fig. 1A–C) across all major cortical and subcortical areas ( $P < 0.05$  false discovery rate [FDR] corrected for all ROIs shown in Fig. 1C); regional BP<sub>ND</sub> values for the three groups are reported in Table 2. BP<sub>ND</sub> in PSP and CBD was 20% to 50% lower than controls ( $P < 0.01$ ), with the most severe median reduction observed in the medulla, substantia nigra, pallidum, midbrain, pons, and caudate nucleus in patients with PSP and in the medulla, hippocampus,

**TABLE 2.** Mean (standard deviation) GTM PVC [<sup>11</sup>C]UCB-J BP<sub>ND</sub> values per group for cortical and subcortical ROIs (surviving FDR correction over 18 regions)

Region	Control	CBD	PSP	F (P)
Frontal lobe	2.96 (0.17)	2.60 (0.29)	2.48 (0.28)	15.05 (<0.0001)
Temporal lobe	2.68 (0.16)	2.30 (0.23)	2.17 (0.27)	19.34 (<0.0001)
Parietal lobe	3.11 (0.19)	2.75 (0.32)	2.63 (0.36)	10.10 (<0.0003)
Occipital lobe	2.98 (0.23)	2.66 (0.29)	2.48 (0.41)	8.80 (0.0008)
Cingulate	3.02 (0.21)	2.56 (0.26)	2.46 (0.28)	20.41 (<0.0001)
Insula	2.76 (0.15)	2.24 (0.26)	2.17 (0.27)	28.55 (<0.0001)
Amygdala	2.71 (0.20)	2.18 (0.34)	2.20 (0.33)	14.67 (<0.0001)
Nucleus accumbens	4.18 (0.31)	3.85 (0.46)	3.54 (0.33)	11.28 (0.0002)
Hippocampus	2.00 (0.20)	1.57 (0.29)	1.57 (0.30)	12.37 (<0.0001)
Caudate nucleus	3.12 (0.22)	2.59 (0.41)	2.48 (0.36)	15.59 (<0.0001)
Pallidum	1.90 (0.22)	1.65 (0.24)	1.27 (0.31)	20.69 (<0.0001) <sup>a</sup>
Putamen	3.99 (0.24)	3.43 (0.32)	3.28 (0.37)	19.94 (<0.0001)
Thalamus	2.86 (0.25)	2.29 (0.45)	2.25 (0.44)	11.23 (<0.0002)
Cerebellum	2.13 (0.22)	1.75 (0.30)	1.69 (0.28)	11.50 (0.0001)
Midbrain	2.61 (0.29)	2.16 (0.38)	1.83 (0.42)	16.61 (<0.0001)
Substantia Nigra	2.13 (0.28)	1.72 (0.34)	1.32 (0.59)	12.79 (<0.0001) <sup>a</sup>
Pons	0.93 (0.13)	0.75 (0.18)	0.71 (0.18)	7.69 (0.002)
Medulla	0.62 (0.16)	0.37 (0.17)	0.28 (0.24)	12.04 (<0.001)

CBD here refers to CBS with a negative amyloid biomarker from [<sup>11</sup>C]PiB PET, and PSP refers to patients with PSP-Richardson's syndrome. F-statistic and P values derived from an ANCOVA across the three groups, with age as a covariate of no interest.

<sup>a</sup>The significant difference here is driven by the PSP group only.

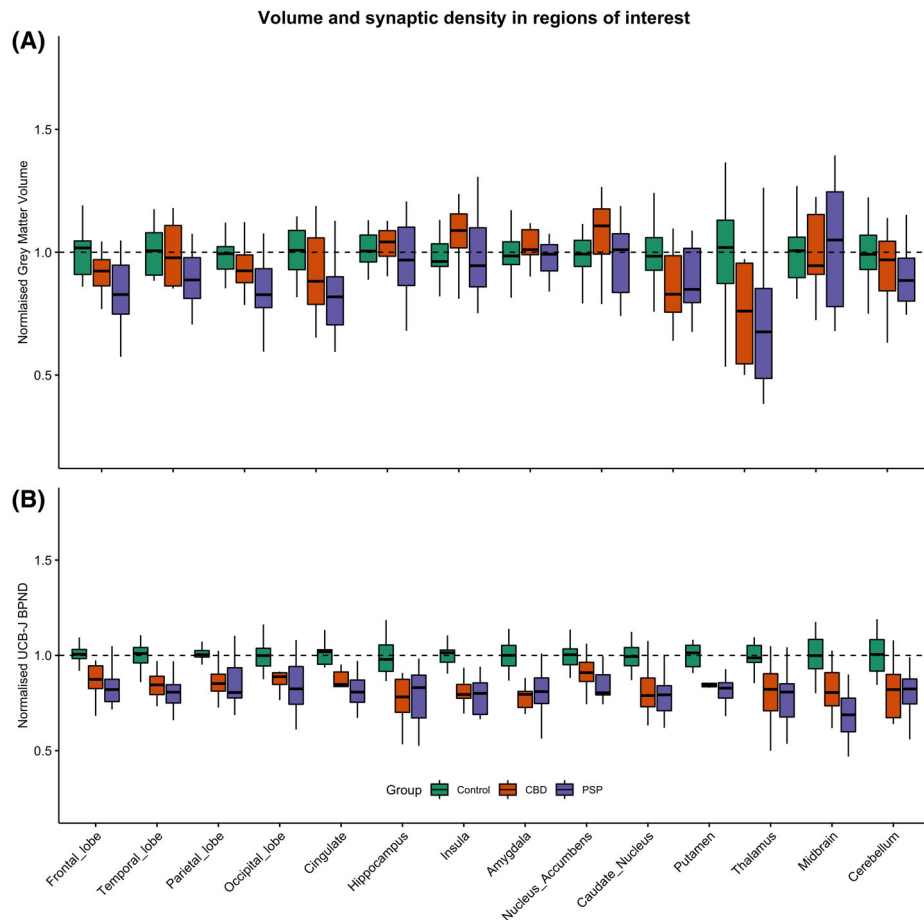


**FIG. 2.** (A) Cortical and subcortical gray matter volumes, normalized against the corresponding volumes in controls, were significantly reduced in the caudate nucleus and thalamus in CBD; and in frontal, temporal, parietal, and occipital lobes, as well as in the caudate nucleus, and thalamus in PSP,  $P < 0.05$ . (B) Mean-centered [<sup>11</sup>C]UCB-J BP<sub>ND</sub> across cortical and subcortical ROIs normalized against the corresponding BP<sub>ND</sub> values in controls, demonstrating a median reduction of 20% to 50%. CBD here refers to CBS with a negative amyloid biomarker from [<sup>11</sup>C]PiB PET, and PSP refers to patients with PSP-Richardson's syndrome.

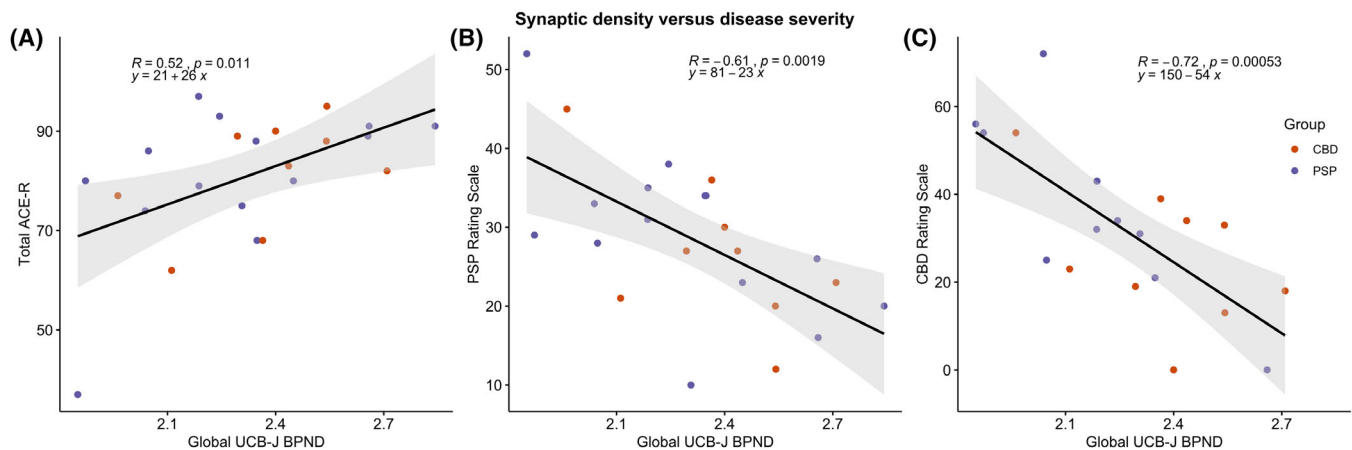


**FIG. 3.** Correlations between global [ $^{11}\text{C}$ ]UCB-J  $\text{BP}_{\text{ND}}$  and total ACE-R score (A), total PSP rating scale (B), and total CBD rating scale (C) for the two patient groups. CBD here refers to CBS with a negative amyloid biomarker from [ $^{11}\text{C}$ ]PiB PET, and PSP refers to patients with PSP-Richardson's syndrome.

amygdala, caudate nucleus, insula, and thalamus in patients with CBD. Post-hoc analysis revealed that the significant differences in  $\text{BP}_{\text{ND}}$  between patients and controls in the pallidum and substantia nigra were mainly driven by the PSP cohort. Using data without GTM PVC, the pattern of statistically significant differences in  $\text{BP}_{\text{ND}}$  for the reported regions in Table 2 remains,  $P < 0.001$ .

The reduction in synaptic density was noted even in areas of the brain that did not show significant gray matter atrophy. Figure 2A shows the group differences in gray matter volume normalized against the mean of the control group; the significant areas of gray matter volume loss were in the caudate nucleus ( $P = 0.01$ ) and thalamus ( $P = 0.04$ ) in the CBD cohort and in the frontal ( $P < 0.01$ ), temporal ( $P = 0.04$ ), parietal ( $P < 0.01$ ), and occipital lobes ( $P < 0.01$ ), caudate nucleus ( $P < 0.001$ ), and thalamus ( $P < 0.01$ ) in the PSP cohort. The reduction in [ $^{11}\text{C}$ ]UCB-J  $\text{BP}_{\text{ND}}$ , however, was more extensive and consistently significantly different across all major cortical and subcortical areas, as shown in the normalized plot in Figure 2B (binding potentials were normalized against the mean binding potential of the control cohort for each ROI).

Correlations between [ $^{11}\text{C}$ ]UCB-J  $\text{BP}_{\text{ND}}$  and both global cognition and disease severity are given in Figure 3. A significant positive correlation was observed between [ $^{11}\text{C}$ ]UCB-J  $\text{BP}_{\text{ND}}$  and the ACE-R total score ( $R = 0.52$ ;  $P = 0.01$ ; Fig. 3A). There was a significant negative correlation between [ $^{11}\text{C}$ ]UCB-J binding and the PSP ( $R = -0.61$ ;  $P < 0.01$ ) and CBD ( $R = -0.72$ ;  $P < 0.001$ ) rating scales (Fig. 3B,C).

## Discussion

The principal result of this study is a widespread reduction in synaptic density in PSP-Richardson's syndrome and amyloid-negative CBS (which we define as

CBD). This accords with postmortem estimates of synaptic loss in PSP and CBD, using synaptophysin immunohistochemistry,<sup>6</sup> imaging of neurite density in PSP,<sup>41</sup> and morphological studies of cortical dendrites in the closely related condition of frontotemporal lobe dementia.<sup>42</sup> Indirect evidence of synaptic loss, from consequential reduction in metabolism, comes from [ $^{18}\text{F}$ ]FDG PET changes in frontal, temporal, and parietal lobes.<sup>43-46</sup> However, PET imaging with the ligand [ $^{11}\text{C}$ ]UCB-J provides direct evidence in vivo of severe and extensive loss of cortical and subcortical synapses, including areas of the brain that are minimally atrophic.<sup>47</sup>

PSP and CBD are progressive, with an average disease duration of 5 to 8 years from symptom onset.<sup>48</sup> In our clinically diagnosed CBD and PSP groups, mean symptom duration at the time of PET was 3.5 years, and our patients were likely to be approximately midway through their symptomatic disease course (not including a potentially long presymptomatic period). The median reduction of 20% (and maximal 50%) in [ $^{11}\text{C}$ ]UCB-J binding observed in vivo, compared to controls, is therefore in keeping with the predictions from postmortem data.

The synaptic loss observed in our study was widespread, extending beyond the regions that are arguably most associated with the diseases. In PSP, from postmortem studies, these include basal ganglia, thalamus, substantia nigra, premotor cortex, as well as the dentate nucleus and cerebellar white matter. In CBD, areas associated with the disease include cortex, thalamus, basal ganglia, and brainstem, without cerebellar involvement.<sup>48-50</sup> However, in our study, the loss of synapses in PSP is global across the cortex, and not confined to the premotor and motor areas, and extends beyond the substantia nigra in the brainstem with pontine and medullary involvement. Loss of synapses in the cerebellum in PSP echoes pathological studies of tau

distribution in this disease.<sup>49</sup> Interestingly, the cerebellum was also markedly abnormal in CBD; although cerebellar atrophy and tau accumulation are not typical associations of CBD.<sup>49</sup> Cerebellar synaptic loss in CBD may therefore represent cerebellar diaschisis in response to widespread cortical pathology and loss of corticocerebellar projections; a small minority of persons in an amyloid-negative CBS cohort may have PSP as the underlying cause for their CBS, although this is unlikely to be sufficient to drive the group-wise effect.

Preclinical models of tauopathy suggest early synaptotoxicity with reduced plasticity and density,<sup>11</sup> in response to soluble oligomeric tau aggregates<sup>12</sup> and inflammation.<sup>51</sup> The toxicity associated with tau pathology leading to synapse loss is complex and involves direct and indirect pathways (reviewed in Spiess-Jones and colleagues<sup>52</sup>). Naturally occurring tau plays a role in synaptic function through modulating microtubule and axonal stability; disruptions to this machinery lead to prevention of the trafficking of essential components to synapses, such as synaptic receptors<sup>53</sup> and mitochondria. Indeed, overexpression of tau interferes with mitochondria transport<sup>54</sup> and contributes to hyperexcitability of neurons and impaired calcium influx in transgenic mouse models (rTg4510).<sup>55</sup> The global nature of synaptic reduction suggests a more widespread pathology in the primary tauopathies of PSP and CBD beyond the areas that are histologically reported as harboring a high tau burden, such as the basal ganglia, thalamus, and brainstem.<sup>56</sup> This may, in part, be explained by the global damage caused by oligomers of tau, which are not easily visible on tau PET imaging or histology. In support of this are biochemical studies that report tau accumulation in both gray and white matter by western blot in PSP, but not necessarily by immunohistochemistry.<sup>57</sup>

We observed a significant correlation between synaptic loss and disease severity in PSP and amyloid-negative CBS. Synaptic loss correlates with cognitive impairment in another clinical tauopathy, AD,<sup>13,58</sup> and preclinical models of this.<sup>59,60</sup> Our *in vivo* PET results support the potential use of synaptic PET as a marker of disease and progression, but longitudinal data are required. Synaptic PET may support early-stage clinical trials in PSP and CBS/CBD; it is encouraging, in this latter respect, that [<sup>11</sup>C]UCB-J PET is sensitive to changes in synaptic density; for example, in response to treatment with the synaptic modulator, Saracatinib.<sup>61</sup>

Our study has several limitations. Although the sample size is small, it is adequately powered in view of the large effect sizes predicted. However, subtler relationships with mild disease, progression, or individual clinical features, or phenotypic variants of PSP and CBS, require larger studies. We acknowledge the potential for off-target binding, but preclinical data indicate very high correlations between UCB-J and synaptophysin, a

marker of presynaptic vesicular density.<sup>25</sup> Our diagnoses were clinical, without neuropathology, although the clinicopathological correlations of PSP-Richardson's syndrome are very high, and in the absence of AD, the clinicopathological correlation of CBS with a 4R-tauopathy (CBD or PSP) is also high.<sup>18</sup> Binding potentials for SV2A radioligands such as [<sup>11</sup>C]UCB-J can be confounded by the use of concurrent medication that may bind to SV2A. We did not enroll any individuals taking levetiracetam or any member of this family of drugs that are SV2A-specific ligands.<sup>62</sup> Previously reported studies using [<sup>11</sup>C]UCB-J in disease have usually not commented on medications used by participants; however, one study using this ligand in major depressive disorders reports exclusion of participants on psychotropic medications in the 2 months preceding PET scanning<sup>63</sup>; whereas many of our PSP and CBD patients are on medications falling under the psychotropic umbrella, to our knowledge, none of these bind to SV2A.

Arterial blood sampling was not carried out in this study; we used reference tissue modeling to reduce the demand on our patient cohort. Reference tissue modeling of [<sup>11</sup>C]UCB-J with the centrum semiovale as the reference tissue has been verified against arterial input function compartmental modeling in healthy controls<sup>39,40</sup> and in AD.<sup>64</sup> To assess the validity of the centrum semiovale in our cohort, we determined the mean total distribution volume ( $V_T$ ) for each of our subject groups using standard arterial input function data from the literature<sup>26,65</sup>; this approach assumed that the standard input function was equally valid for all groups. This analysis indicated a small positive bias in centrum semiovale  $V_T$  for CBD (5%) and less so PSP (2%) relative to that in controls, which would lead to a commensurate reduction in  $BP_{ND}$  under the assumption that the nondisplaceable distribution volume in the target ROIs remains invariant. These biases cannot, however, explain the much greater  $BP_{ND}$  reductions observed for CBD and PSP, which is especially true for PSP. Indeed, scaling  $BP_{ND}$  in the CBD and PSP cohorts to account for the above biases in centrum semiovale  $V_T$  produced a similar pattern of significant global reduction in  $BP_{ND}$  for patients compared to controls, except that the significant differences in the midbrain, pons, substantia nigra, pallidum, and occipital lobe were primarily driven by the PSP cohort in the post-hoc analysis.

The therapeutic challenge in tauopathies is partly attributable to the complex nature of the underlying pathology. Early-stage trials will require early accurate diagnosis, although diagnosis is typically made 3 years after symptom onset.<sup>66,67</sup> It is unlikely that synaptic PET could provide presymptomatic diagnosis in rare conditions, but it is a promising tool to characterize pathogenetic mechanisms, monitor progression, and assess response to experimental medicines.<sup>68</sup> ■

**Acknowledgements:** We thank the participants, the staff at the Wolfson Brain Imaging Centre, and the staff at the Cambridge Centre for Parkinson-Plus. We thank the NIHR Cambridge Biomedical Research Centre for Support.

## References

- Armstrong MJ, Litvan I, Lang AE, et al. Criteria for the diagnosis of corticobasal degeneration. *Neurology* 2013;80:496–503.
- Burrell JR, Hodges JR, Rowe JB. Cognition in corticobasal syndrome and progressive supranuclear palsy: a review. *Mov Disord* 2014;29:684–693.
- Höglinger GU, Respondek G, Stamelou M, et al. Clinical diagnosis of progressive supranuclear palsy: the Movement Disorder Society criteria. *Mov Disord* 2017;32:853–864.
- Litvan I, Agid Y, Calne D, et al. Clinical research criteria for the diagnosis of progressive supranuclear palsy (Steele-Richardson-Olszewski syndrome): report of the NINDS-SPSP International Workshop. *Neurology* 1996;47:1–9.
- Rösler TW, Tayanian Marvian A, Brendel M, et al. Four-repeat tauopathies. *Prog Neurobiol* 2019;180:101644.
- Bigio EH, Vono MB, Satumtira S, et al. Cortical synapse loss in progressive supranuclear palsy. *J Neuropathol Exp Neurol* 2001;60:403–410.
- Lipton AM, Munro Cullum C, Satumtira S, et al. Contribution of asymmetric synapse loss to lateralizing clinical deficits in frontotemporal dementias. *Arch Neurol* 2001;58:1233–1239.
- Foster NL, Minoshima S, Johanns J, et al. PET measures of benzodiazepine receptors in progressive supranuclear palsy. *Neurology* 2000;54:1768–1773.
- Andersson JD, Matuskey D, Finnema SJ. Positron emission tomography imaging of the  $\gamma$ -aminobutyric acid system. *Neurosci Lett* 2019;691:35–43.
- Jiang S, Wen N, Li Z, et al. Integrative system biology analyses of CRISPR-edited iPSC-derived neurons and human brains reveal deficiencies of presynaptic signaling in FTL and PSP. *Transl Psychiatry* 2018;8:265.
- Menkes-Caspi N, Yamin HG, Kellner V, Spires-Jones TL, Cohen D, Stern EA. Pathological tau disrupts ongoing network activity. *Neuron* 2015;85:959–966.
- Kaniyappan S, Chandupatla RR, Mandelkow EM, Mandelkow E. Extracellular low-n oligomers of tau cause selective synaptotoxicity without affecting cell viability. *Alzheimers Dement* 2017;13:1270–1291.
- Terry RD, Masliah E, Salmon DP, et al. Physical basis of cognitive alterations in Alzheimer's disease: synapse loss is the major correlate of cognitive impairment. *Ann Neurol* 1991;30:572–580.
- Gazzina S, Respondek G, Compta Y, et al. Neuropathological validation of the MDS-PSP criteria with PSP and other frontotemporal lobar degeneration. *bioRxiv* 2019 Jan 15. doi: <https://doi.org/10.1101/520510>. Article posted for preprint.
- Steele JC, Richardson JC, Olszewski J. Progressive supranuclear palsy: a heterogeneous degeneration involving the brain stem, basal ganglia and cerebellum with vertical gaze and pseudobulbar palsy, nuchal dystonia and dementia. *Arch Neurol* 1964;10:333–359.
- Williams DR, Lees AJ. Progressive supranuclear palsy: clinicopathological concepts and diagnostic challenges [Internet]. Vol. 8, *The Lancet Neurology*. 2009;8:270–279.
- Burrell JR, Hodges JR, Rowe JB. Cognition in corticobasal syndrome and progressive supranuclear palsy: a review. *Mov Disord* 2014;29:684–693.
- Alexander SK, Rittman T, Xuereb JH, Bak TH, Hodges JR, Rowe JB. Validation of the new consensus criteria for the diagnosis of corticobasal degeneration. *J Neurol Neurosurg Psychiatry* 2014;85:923–927.
- Jabbari E, Holland N, Chelban V, et al. Diagnosis across the spectrum of progressive supranuclear palsy and corticobasal syndrome. *JAMA Neurol* 2019 Dec 20. doi: <https://doi.org/10.1001/jamaneurol.2019.4347>. [Epub ahead of print]
- Sami S, Williams N, Hughes LE, et al. Neurophysiological signatures of Alzheimer's disease and frontotemporal lobar degeneration: pathology versus phenotype. *Brain* 2018;141:2500–2510.
- Cope TE, Rittman T, Borchert RJ, et al. Tau burden and the functional connectome in Alzheimer's disease and progressive supranuclear palsy. *Brain* 2018;141:550–567.
- Hughes LE, Rowe JB, Ghosh BCP, Carlyon RP, Plack CJ, Gockel HE. The binaural masking level difference: Cortical correlates persist despite severe brain stem atrophy in progressive supranuclear palsy. *J Neurophysiol* 2014;112:3086–3094.
- Wolpe N, Moore JW, Rae CL, et al. The medial frontal-prefrontal network for altered awareness and control of action in corticobasal syndrome. *Brain* 2014;137:208–220.
- Milicevic Sephton S, Miklovicz T, Russell J, Doke A, Li L, Boros I. Automated radiosynthesis of [ $^{11}\text{C}$ ]UCB-J for imaging synaptic density by PET. *J Label Compd Radiopharm* 2020. doi: <https://doi.org/10.17863/CAM.48002>. [Epub ahead of print]
- Finnema SJ, Nabulsi NB, Eid T, et al. Imaging synaptic density in the living human brain. *Sci Transl Med* 2016;8:348ra96.
- Finnema SJ, Nabulsi NB, Mercier J, et al. Kinetic evaluation and test-retest reproducibility of [ $^{11}\text{C}$ ]UCB-J, a novel radioligand for positron emission tomography imaging of synaptic vesicle glycoprotein 2A in humans. *J Cereb Blood Flow Metab* 2018;38:2041–2052.
- Bajjalieh SM, Peterson K, Linial M, Scheller RH. Brain contains two forms of synaptic vesicle protein 2. *Proc Natl Acad Sci U S A* 1993;90:2150–2154.
- Bajjalieh SM, Frantz GD, Weimann JM, McConnell SK, Scheller RH. Differential expression of synaptic vesicle protein 2 (SV2) isoforms. *J Neurosci* 1994;14:5223–5235.
- Chen MK, Mecca AP, Naganawa M, et al. Assessing synaptic density in Alzheimer disease with synaptic vesicle glycoprotein 2A positron emission tomographic imaging. *JAMA Neurol* 2018;75:1215–1224.
- Klunk WE, Koeppe RA, Price JC, et al. The Centiloid project: standardizing quantitative amyloid plaque estimation by PET. *Alzheimers Dement* 2015;11:1–15.e4.
- Jack CR, Wiste HJ, Weigand SD, et al. Defining imaging biomarker cut points for brain aging and Alzheimer's disease. *Alzheimers Dement* 2017;13:205–216.
- Milicevic Sephton S, Miklovicz T, Russell JJ, et al. Automated radiosynthesis of [ $^{11}\text{C}$ ]UCB-J for imaging synaptic density by positron emission tomography. *J Label Compd Radiopharm* 2020;63:151–158.
- Burgos N, Cardoso MJ, Thielemans K, et al. Attenuation correction synthesis for hybrid PET-MR scanners: application to brain studies. *IEEE Trans Med Imaging*. 2014; 33:2332–2341.
- Prados F, Cardoso MJ, Burgos N, et al. NiftyWeb: web based platform for image processing on the cloud. In: 24th Scientific Meeting and Exhibition of the International Society for Magnetic Resonance in Medicine (ISMRM), Singapore, 7–13 May 2016.
- Manavaki R, Hong Y, Fryer TD. Brain MRI coil attenuation map processing for the GE SIGNA PET/MR: impact on PET image quantification and uniformity. In: IEEE Nuclear Science Symposium. (NSS) and Medical Imaging Conference, Manchester, UK, 26 October to November 2, 2019.
- Avants BB, Epstein CL, Grossman M, Gee JC. Symmetric diffeomorphic image registration with cross-correlation: evaluating automated labeling of elderly and neurodegenerative brain. *Med Image Anal* 2008;12:26–41.
- Rousset OG, Ma Y, Evans AC. Correction for partial volume effects in PET: principle and validation. *J Nucl Med*. 1998;39:904–911.
- Wu Y, Carson RE. Noise reduction in the simplified reference tissue model for neuroreceptor functional imaging. *J Cereb Blood Flow Metab*. 2002;22:1440–1452.
- Koole M, van Aalst J, Devrome M, et al. Quantifying SV2A density and drug occupancy in the human brain using [ $^{11}\text{C}$ ]UCB-J PET imaging and subcortical white matter as reference tissue. *Eur J Nucl Med Mol Imaging* 2019;46:396–406.
- Rossano S, Toyonaga T, Finnema SJ, et al. Assessment of a white matter reference region for  $^{11}\text{C}$ -UCB-J PET quantification. *J Cereb*

- Blood Flow Metab. 2019 Sep 30. doi: <https://doi.org/10.1177/0271678X19879230>. [Epub ahead of print]
41. Mitchell T, Archer DB, Chu WT, et al. Neurite orientation dispersion and density imaging (NODDI) and free-water imaging in Parkinsonism. *Hum Brain Mapp* 2019;40:5094–5107.
  42. Ferrer I, Roig C, Espino A, et al. Dementia of frontal lobe type and motor neuron disease. A Golgi study of the frontal cortex. *J Neurol Neurosurg Psychiatry* 1991;54:932–934.
  43. Juh R, Kim J, Moon D, Choe B, Suh T. Different metabolic patterns analysis of Parkinsonism on the 18 F-FDG PET. *Eur J Radiol* 2004;54:223–233.
  44. Blin J, Vidailhet MJ, Pillon B, Dubois B, Fève JR, Agid Y. Corticobasal degeneration: decreased and asymmetrical glucose consumption as studied with PET. *Mov Disord* 1992;7:348–354.
  45. Eidelberg D, Dhawan V, Moeller JR, et al. The metabolic landscape of cortico-basal ganglionic degeneration: regional asymmetries studied with positron emission tomography. *Neurosurg Psychiatry* 1991;54:856–862.
  46. Foster NL, Gilman S, Berent S, Morin EM, Brown MB, Koeppe RA. Cerebral hypometabolism in progressive supranuclear palsy studied with positron emission tomography. *Ann Neurol* 1988;24:399–406.
  47. Josephs KA, Whitwell JL, Dickson DW, et al. Voxel-based morphometry in autopsy proven PSP and CBD. *Neurobiol Aging* 2008;29:280–289.
  48. Dickson DW, Bergeron C, Chin SS, et al. Office of Rare Diseases neuropathologic criteria for corticobasal degeneration. *J Neuropathol Exp Neurol* 2002;61:935–946.
  49. Dickson DW, Kouri N, Murray ME, Josephs KA. Neuropathology of frontotemporal lobar degeneration-Tau (FTLD-Tau). *J Mol Neurosci* 2011;45:384–389.
  50. Kovacs GG, Lukic MJ, Irwin DJ, et al. Distribution patterns of tau pathology in progressive supranuclear palsy. *Acta Neuropathol* 2020 May 7. doi: <https://doi.org/10.1007/s00401-020-02158-2>. [Epub ahead of print]
  51. Rajendran L, Paolicelli RC. Microglia-mediated synapse loss in Alzheimer's disease. *J Neurosci* 2018;38:2911–2919.
  52. Spires-Jones TL, Hyman BT. The intersection of amyloid beta and tau at synapses in Alzheimer's disease. *Neuron* 2014;82:756–771.
  53. Hoover BR, Reed MN, Su J, et al. Tau mislocalization to dendritic spines mediates synaptic dysfunction independently of neurodegeneration. *Neuron* 2010;68:1067–1081.
  54. Stoothoff W, Jones PB, Spires-Jones TL, et al. Differential effect of three-repeat and four-repeat tau on mitochondrial axonal transport. *J Neurochem* 2009;111:417–427.
  55. Rocher AB, Crimins JL, Amatrudo JM, et al. Structural and functional changes in tau mutant mice neurons are not linked to the presence of NFTs. *Exp Neurol* 2010;223:385–393.
  56. Dickson DW, Kouri N, Murray ME, Josephs KA. Neuropathology of frontotemporal lobar degeneration-Tau (FTLD-Tau). *J Mol Neurosci* 2011;45:384–389.
  57. Zhukareva V, Joyce S, Schuck T, et al. Unexpected abundance of pathological tau in progressive supranuclear palsy white matter. *Ann Neurol* 2006;60:335–345.
  58. Robinson JL, Molina-Porcel L, Corrada MM, et al. Perforant path synaptic loss correlates with cognitive impairment and Alzheimer's disease in the oldest-old. *Brain* 2014;137:2578–2587.
  59. Kandimalla R, Manczak M, Yin X, Wang R, Reddy PH. Hippocampal phosphorylated tau induced cognitive decline, dendritic spine loss and mitochondrial abnormalities in a mouse model of Alzheimer's disease. *Hum Mol Genet* 2018;27:30–40.
  60. Walsh DM, Klyubin I, Fadeeva JV, et al. Naturally secreted oligomers of amyloid  $\beta$  protein potently inhibit hippocampal long-term potentiation in vivo. *Nature* 2002;416:535–539.
  61. Toyonaga T, Smith LM, Finnema SJ, et al. In vivo synaptic density imaging with <sup>11</sup>C-UCB-J detects treatment effects of saracatinib (AZD0530) in a mouse model of Alzheimer's disease. *J Nucl Med* 2019;60:1780–1786.
  62. Löscher W, Gillard M, Sands ZA, Kaminski RM, Klitgaard H. Synaptic vesicle glycoprotein 2A ligands in the treatment of epilepsy and beyond. *CNS Drugs* 2016;30:1055–1077.
  63. Holmes SE, Scheinost D, Finnema SJ, Naganawa M, Davis MT, DellaGioia N, et al. Lower synaptic density is associated with depression severity and network alterations. *Nat Commun* 2019;10:1529.
  64. Chen MK, Mecca AP, Naganawa M, et al. Assessing synaptic density in Alzheimer disease with synaptic vesicle glycoprotein 2A positron emission tomographic imaging. *JAMA Neurol* 2018;75:1215–1224.
  65. Mansur A, Rabiner EA, Comley RA, et al. Characterization of 3 PET tracers for quantification of mitochondrial and synaptic function in healthy human brain: <sup>18</sup>F-BCPP-EF, <sup>11</sup>C-SA-4503, and <sup>11</sup>C-UCB-J. *J Nucl Med* 2020;61:96–103.
  66. Mamarabadi M, Razjouyan H, Golbe LI. Is the latency from progressive supranuclear palsy onset to diagnosis improving? *Mov Disord Clin Pract* 2018;5:603–606.
  67. Coyle-Gilchrist ITS, Dick KM, Patterson K, et al. Prevalence, characteristics, and survival of frontotemporal lobar degeneration syndromes. *Neurology* 2016;86:1736–1743.
  68. Cai Z, Li S, Matuskey D, Nabulsi N, Huang Y. PET imaging of synaptic density: a new tool for investigation of neuropsychiatric diseases. *Neurosci Lett* 2019;691:44–50.

## Supporting Data

Additional Supporting Information may be found in the online version of this article at the publisher's web-site.

SGML and CITI Use Only  
DO NOT PRINT

Author Roles

(1) Research Project: A. Conception, B. Organization, C. Execution; (2) Statistical Analysis: A. Design, B. Execution, C. Review and Critique; (3) Manuscript: A. Writing of the First Draft, B. Review and Critique.

N.H.: 1A, 1B, 1C, 2A, 2B, 2C, 3A, 3B

P.S.J.: 2C, 3B

G.S.: 1B, 1C, 3B

J.K.W.: (1B, 1C, 3B

Y.T.H.: 1C, 2C, 3B

T.D.F.: 2C, 3B

R.M.: 1C, 2C

S.M.-S.: 1C, 3B

I.B.: 3C

M.M.: 2C, 3B

F.H.H.: 2B, 3B

F.I.A.: 1A, 3B

J.P.C.: 1A, 3B

J.O.B.: 1A, 2C, 3B

J.B.R.: 1A, 2C, 3B

Financial Disclosures

N.H. is funded by the Association of British Neurologists–Patrick Berthoud Charitable Trust. J.B.R. serves as an associate editor to *Brain* and is a nonremunerated trustee of the Guarantors of Brain and the PSP Association (UK). He provides consultancy to Asceneuron, Biogen, and UCB and has research grants from AZ-Medimmune, Janssen, and Lilly as industry partners in the Dementias Platform UK. J.O.B. provides consultancy to Axon, TauRx, and Eisai and has research grant support from Alliance Medical and Merck. F.I.A. receives financial support and material (ligand precursor) from UCB Pharma.